GEOLOGICA CARPATHICA, AUGUST 2015, 66, 4, 303–310 doi: 10.1515/geoca-2015-0027

The origin of native selenium microparticles during the oxidation of sideritic mudstones in the Veřovice Formation (Outer Western Carpathians)

DALIBOR MATÝSEK and PETR SKUPIEN

Institute of Geological Engineering, VŠB — Technical University of Ostrava, 17. listopadu 15, 708 33 Ostrava-Poruba, Czech Republic; dalibor.matysek@vsb.cz; petr.skupien@vsb.cz

(Manuscript received December 1, 2014; accepted in revised form June 23, 2015)

Abstract: Microparticles of native selenium were detected in weathered sideritic mudstones of the Veřovice Formation (Aptian) of the Silesian Unit (Outer Western Carpatians, NE part of the Czech Republic). This mineral forms small needle-like crystals with lengths of up to 20 μm, and is confined to fissures in sideritic mudstones covered by goethite or rarely also by hydrated Mn-oxide minerals. The oxidized sideritic mudstones show zonal structure and resemble the initial stage of the formation of the so-called rattle stones. From the superposition of phase diagrams of selenium and Fe-oxyhydroxides, Fe apparently occupies a large field in which Se(0) and FeOOH and/or $Fe(OH)_3$ can co-exist. The reduction of selenites or selenates by pyrite or by any other phase, capable of charge transfer, is likely to have been responsible for the formation of microparticles of native selenium. The crucial factor controlling the origin of these particles is the extremely low solubility of Se(0). The source of Se is not obvious. It can be released in trace concentrations during the weathering of pyrite. Sediments of the Veřovice Formation correspond to the anoxic event OAE1b and accumulation of siderophile elements in similar sediments is very probable. A probable mechanism for the origin of Se microcrystals is gradual crystallization from solution.

Key words: Western Carpathians, Lower Cretaceous, sideritic mudstones, native selenium.

Introduction

When studying the mineralogy of the products of weathering of bedded sideritic mudstones in the Czech part of the Moravian-Silesian Beskydy Mountains (Fig. 1) some microparticles consisting of native selenium were detected in fissures of these sediments. Native selenium is a relatively rare mineral that is bound by its origin mainly to the oxidation of Se-rich organic matter in sandstones of uranium and uranium-vanadium mineral deposits, to the sublimation products of volcanic fumaroles and to gaseous products of burning heaps from coal mining (Anthony et al. 1990; Jianming et al. 2004). The mineral is trigonal trapezohedral with space group $P3_121$ or $P3_221$ (Anthony et al. 1990). It usually forms opaque needle-like crystals. Selenium is an essential biogenic microelement that shows considerable toxicity at only slightly higher concentrations. Its geochemical behaviour in the geosphere has been summarized by Malisa (2001), Plant (2013), and in soil by Strawn et al. (2002) and by Tolu et al. (2014).

The occurrence of native selenium in common sedimentary sequences is an interesting finding that requires clarification of the conditions controlling its formation. If a more common occurrence of this mineral is proved, then models of the geochemical behaviour and character of selenium in the process of weathering will have to be modified and the possibility of its accumulation in the form of Se(0) needs to be taken into account.

There is only minimal data in the literature on the occurrence of native Se in sedimentary sequences or about its origin during the process of weathering. In the area of the Western Carpathians there is only one reference to the occurrence of microparticles of selenium sitting on a crystal of pyrite (Szełęg et al. 2013). Here selenium forms needle-like crystals with a maximum length of 30 μm growing together with barite on a (001) crystal plane of partly oxidized pyrite about 4 mm in size. This occurrence comes from low-temperature hydrothermal veins of the Godula Formation of the Silesian Unit (Senonian). The aim of the paper is to document two new occurrences of native selenium in sideritic mudstones of the Veřovice Formation, Outer Western Carpathians and to discuss their origin.

Methods of investigation

The crystals of selenium were identified during a brief study of the products of weathering of sideritic mudstones using electron microscopy and energy dispersive microanalysis carried out on untreated flat samples. The nature of the crystals does not allow preparation of polished thin sections or their metal coating using the sputtering process in a plasma environment. It was also found that, when carrying out electron probe microanalyses, some damage to analysed grains may occur including their burning through, which leads during the analysis to a gradual increase in the content of elements originating from the substrate, which may not be present in the analysed grains. These mainly include the contents of oxygen and iron and/or manganese. A typical EDX

(Energy Dispersive X-ray Spectroscopy) spectrum of selenium particles is shown in Fig. 2. Therefore, the only available solution is to minimize the time needed to carry out the EDX analysis. The WDA analyses (Wave dispersion) do not provide reliable results. The crystals of selenium can be removed by simple washing of the samples.

The electron microscopy and EDX microanalyses were performed on a FEI Quanta-650 FEG instrument equipped with EDAX detectors — EDAX Galaxy, WDA-EDAX LEXS, EBSD-EDAX TSL and CL — Gatan MonoCL4. The energy dispersive microanalysis carried out under the above conditions must be considered only semi-quantitative. Only simple analyses without using appropriate standards were carried out but applying correction of the contents of light elements on the basis of a set of standard materials under the following conditions: voltage 15 kV, current of 8–10 nA, beam diameter

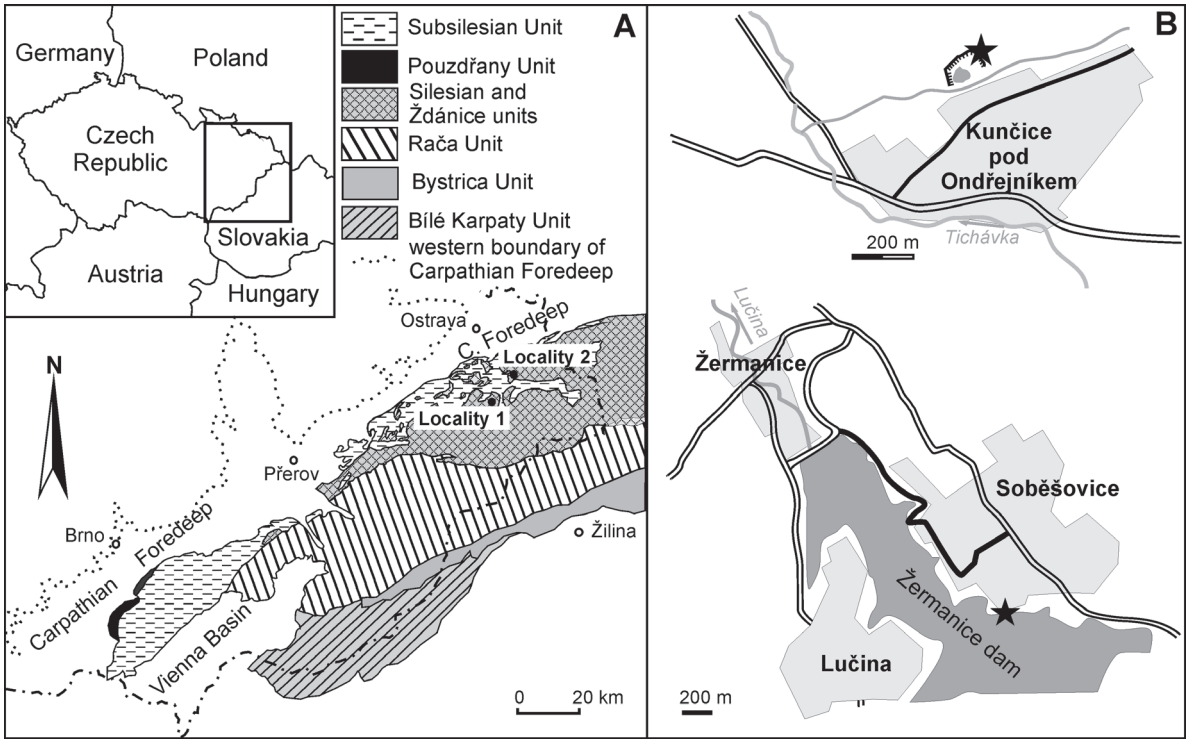

Fig. 1. A — Tectonic map of the Outer Western Carpathian area of the Czech Republic with localities, **B** — Location of the discoveries of the native selenium: locality 1 — Kunčice pod Ondřejníkem, locality 2 — Soběšovice.

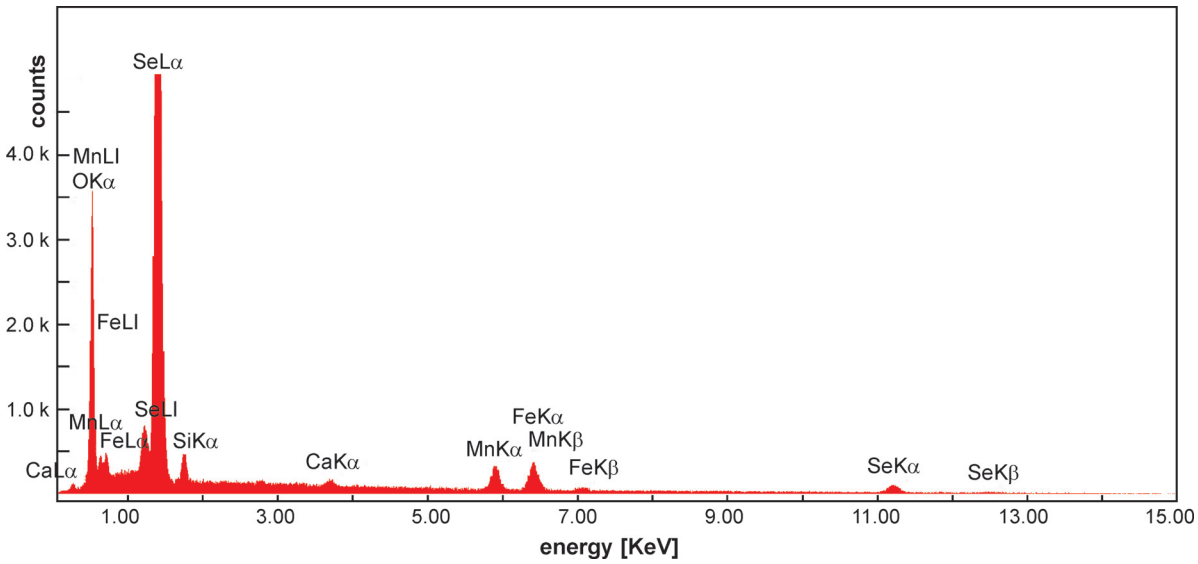

Fig. 2. A characteristic EDX spectrum taken on the crystal plane of a selenium particle. In addition to the dominant lines of Se, lines of Fe, Mn, Ca and O are also present, which come from the substrate of the crystal. Locality 2 (Soběšovice).

5.5 μm, reduced pressure in the vacuum chamber 50 Pa, samples without coating.

Powder X-ray diffraction analyses were carried out to characterize the overall composition of the samples and to identify the products of weathering of sideritic mudstones. Analyses were made on a Bruker-AXS D8 Advance instrument with 2θ/θ reflection geometry measurements, equipped with a semiconductor — silicon strip detector- model LynxEye. Measurements were carried out under the following conditions: radiation CoKα/Fe, voltage 40 kV, current 40 mA, step mode with a step of 0.014 2θ, time at step 0.25 sec., summation of 3–5 measurements, the angle range 5–80° 2θ. Software Bruker — AXS Diffrac or Diffrac. EVA and database of diffraction data PDF 2/JCPDS, version 2011 were used for the measurements and qualitative evaluation of the obtained values. A semi-quantitative evaluation was performed by means of the Rietveld method and using the program TOPAS, version 4.2. Input structural data were taken from the Bruker Structural Database. Both electron microscopy and XRD analysis were performed in the laboratories of Institute of Clean Technologies for Mining and Utilization of Raw Material for Energy Use (VŠB-TU Ostrava, Faculty of Mining and Geology).

Geological setting and description of the identified mineralization

Microparticles of selenium were found at two localities (Fig. 1). Locality 1 lies in the cadastre of the Kunčice pod Ondřejníkem village (GPS 49°32′46.313″ N, 18°16′33.461″ E) and is represented by the NE wall of an abandoned and partially flooded quarry (Fig. 1). Locality 2 is situated on the cadastral boundary of the municipalities of Lučina and Soběšovice (GPS 49°43′18.012″ N, 18°27′53.240″ E). This is a flat outcrop on the beach of the Žermanice dam (Fig. 1) only exposed at low water levels.

Both studied localities represent outcrops which by microfossil dating belong to the Veřovice Formation of the Sile-

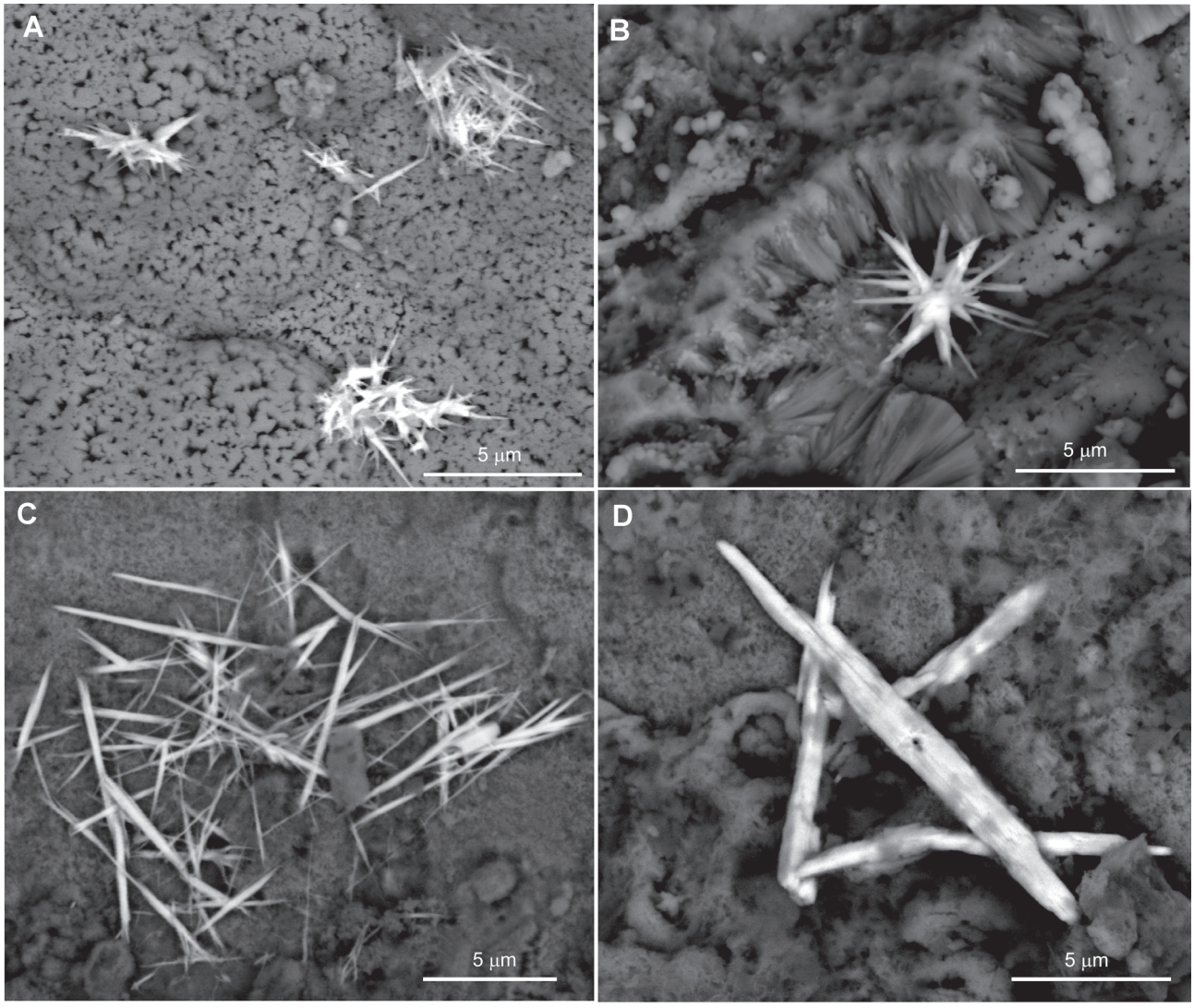

Fig. 3. Morphology of selenium crystals on the surface of fissures in slightly weathered sideritic mudstones. BSE images. **A, B** — Locality Kunčice pod Ondřejníkem, **C, D** — Locality Soběšovice.

sian Unit affected by weathering in the deeper parts of the soil profile. There are black and grey, usually strongly silicified aleurites and pelites with accessoric proportion of beds of sideritic mudstones or sandstones. Judging from the identified non-calcareous dinoflagellates, the local sediments are of Aptian age (pers. obs. Skupien) or more accurately belong to the latest Aptian. Sediments of the Veřovice Formation are characterized by their non-calcareous nature, but otherwise are rich in organic carbon (TOC 2–3.5 wt. % — Pavluš & Skupien 2014). The conditions during sedimentation can be associated with an anoxic environment, and the Veřovice Formation can be correlated with the oceanic anoxic event designated as OAE1b (Skupien et al. 2013; Kaim et al. 2013).

Samples at both localities were taken from a depth of about 1.5–2 m below the present surface. The exposed section at both sites is very similar. It consists of isolated beds of sideritic mudstone 10–20 cm thick, enclosed in black-grey, crispy aleurites and pellites that disintegrated into blocks or cubes. The beds of mudstones were tectonically segmented into polygonal, generally wedge-shaped fragments of a size of 20×20 cm. These sediments suffered from strong weathering along the primary jointing that is manifested by a significant concentric structure of the fragments.

Results

Microparticles of native selenium identified by EDX spectra (Fig. 2) occur in the form of very thin, needle-like crystals and their aggregates on the surface of fissures in weathered sideritic mudstones. The crystals always occur on a coating formed by oxyhydroxides of Fe (goethite), and also rarely as at locality 2 (Soběšovice), on thin lamellar coatings of hydrated Mn-oxide minerals. Needles of selenium occur either as isolated crystals or are intergrown to form bundles and aggregates (Fig. 3). Only rarely is it possible to observe signs of hexagonal crystal planes. The crystals are rarely 20 μm long, but usually are max. 5 μm in size. The thickness of crystals ranges in general in tenths of a micrometer, max. 0.5–1 μm.

Associated minerals in mudstone fissures

Microparticles of selenium in the fissures of sideritic mudstones at both localities are associated with goethite forming coatings consisting of irregularly lobated particles, fibres and needle-like crystals. At Kunčice pod Ondřejníkem relatively abundant barite occurs in the form of tabular crystals up to 2 μm in size (Fig. 4A). Rare black, highly vitreous coatings of lepidocrocite form of prismatic crystals have max. 5 μm (Fig. 4B). Hydrated Mn oxide minerals, specifically todorokite and lithiophorite (Fig. 4C) were identified in separate fissures. Todorokite forms coatings comprising intergrowths of extremely thin tabular crystals, whereas lithiophorite occurs as globular aggregates consisting of oriented intergrowths of pseudohexagonal tabular crystals and was found only rarely. Both hydrated oxide minerals of Mn and Fe, as well as lepidocrocite were detected and proved by powder X-ray diffraction. The main diffraction lines and refined cell dimensions for hydrated Mn-oxide minerals are shown in Table 1.

EDX microanalysis of the lithiophorite [$(Al, Li)Mn^{4+}O_2(OH)_2$] displays a high content of Al. With regard to the fact that electron microanalysis does not allow the determination of Li, one cannot comment more closely on the content and behaviour of

Table 1: Main diffraction lines and refined cell dimensions of manganese and iron minerals from weathered sideritic mudstones.

Lithiophorite — Kunčice p. Ondřejníkem locality
Diffraction lines (hkl – d [nm]): (003) – 0. 9483; (006) – 0.7417; (009) – 0.31611; (00–12) – 0.5496; (00–15) – 0.1897
Refined cell parameters: a_0 = 0.29275(35) nm, c_0 = 2.8450(10) nm
Published cell parameters for comparison (Post & Appleman 1994): a_0 = 0.29247(4), c_0 = 2.8169(6) nm
Todorokite — Kunčice p. Ondřejníkem locality
Diffraction lines (hkl – d [nm]): (100) – 1.05169; (001) – 0.94812; (002) – 0.47406; (003) – 0.31604
Refined cell parameters: a_0 = 1.0055(5), b_0 = 0.2723(11), c_0 = 0.9511(14) nm, β = 94.53(33)°
Published cell parameters for comparison (Post et al. 2003): a_0 = 0.9769, b_0 = 0.28512, c_0 = 0.9560 nm, β = 94.47°
Manganite — Soběšovice locality
Diffraction lines (hkl – d [nm]): (1–1–1) – 0.34077; (020) – 0.2397; (111) – 0.25243; (200) – 0.24162; (1–2–1) – 0.22718; (022) – 0.17822
Refined cell parameters (in space group $P2_1/c$): a_0 = 0.53071(33), b_0 = 0.52794(7), c_0 = 0.53071(60) nm, β = 114.42(16)°
Published cell parameters for comparison (PDF 60-041-1379, $P2_1/c$): a_0 = 0.5300, b_0 = 0.5278, c_0 = 0.5307 nm, β = 114.36(16)°
Pyrolusite — Soběšovice locality
Diffraction lines (hkl – d [nm]): (110) – 0.31211; (011) – 0.24032; (020) – 0.22070; (211) – 0.16255
Refined cell parameters: a_0 = 0.4414(2), c_0 = 0.2865(4) nm
Published cell parameters for comparison (PDF 00-024-0735): a_0 = 0.4399, c_0 = 0.2874 nm
Lepidocrocite — Kunčice p. Ondřejníkem locality
Diffraction lines (hkl – d [nm]): (020) – 0.62611; (021) – 0.32934; (130) – 0.24725, (150) – 0.19403; (151) – 0.17347
Refined cell parameters: a_0 = 0.306886(7), b_0 = 1.25221(3), c_0 = 0.38724(1) nm
Published cell parameters for comparison (PDF 01-070-8045): a_0 = 0.3072, b_0 = 1.2516, c_0 = 0.388 nm
Goethite — Kunčice p. Ondřejníkem locality
Diffraction lines (hkl – d [nm]): (101) – 0.41805; (301) – 0.26925; (210) – 0.25822; (111) – 0.24482; (211) – 0.22524 nm
Refined cell parameters: a_0 = 0.9955(2), b_0 = 0.30204(5), c_0 = 0.46063(8) nm
Published cell parameters for comparison (Yang et al. 2006): a_0 = 0.9951, b_0 = 0.30178, c_0 = 0.45979 nm

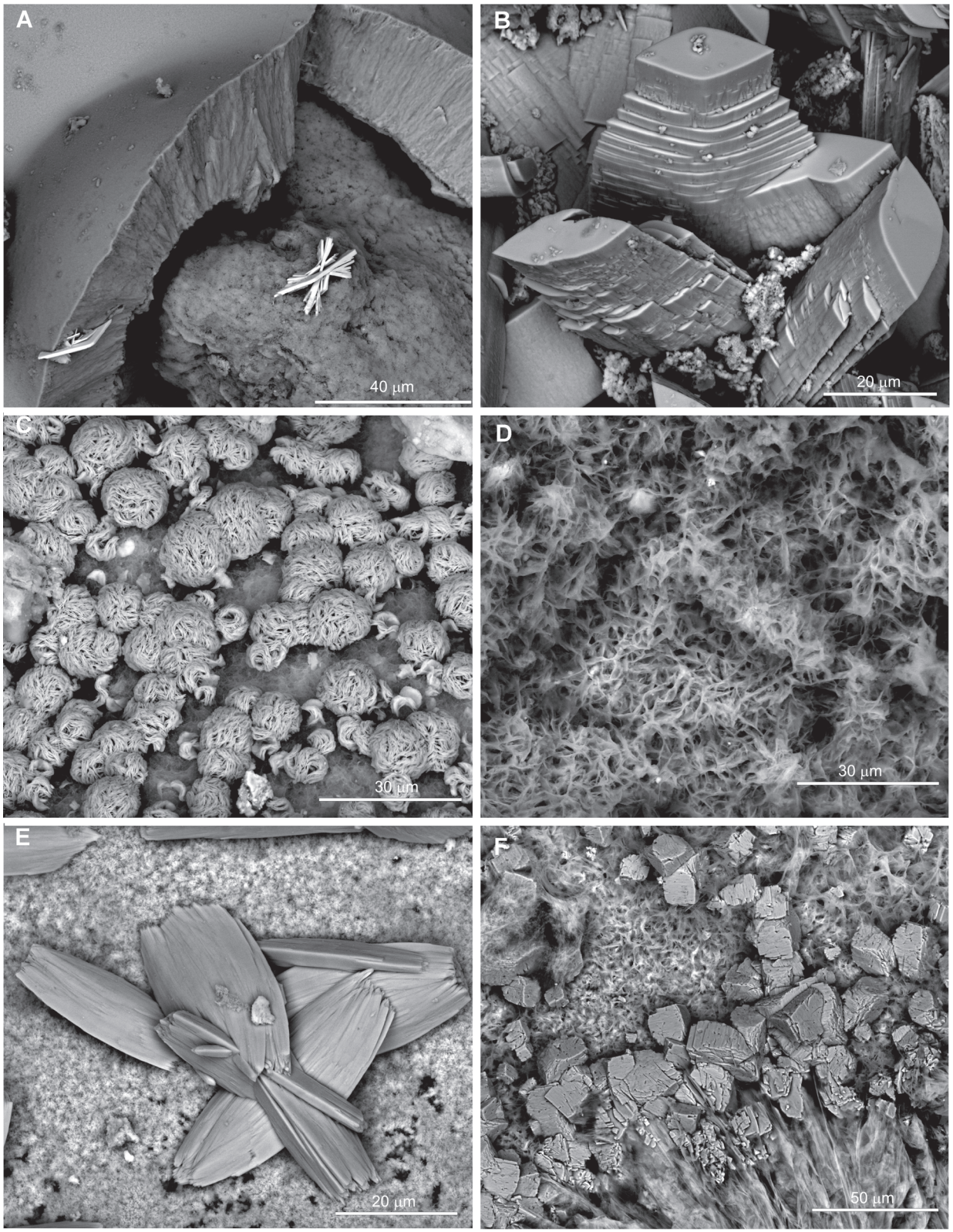

Fig. 4. Morphology of minerals accompanying selenium in fissures of slightly weathered sideritic mudstones from the locality Kunčice pod Ondřejníkem (A–C) and locality Soběšovice (D–F). **A** — Aggregates of barite in massive coating formed by goethite, **B** — Detail of lepidocrocite crystals, **C** — Spherical aggregates consist of intergrown tabular crystals of lithiophorite, **D** — Detail of aggregates of hydrated Mn- oxide mineral, consisting of intergrown and deformed very thin tabular grains, **E** — Detail of crystal aggregates of manganite, **F** — An aggregate of prismatic crystals of pyrolusite along with an unidentified hydrated Mn- oxide mineral, which forms very thin curled tabular grains in the bottom of the picture.

this element in the localities under study. Todorokite is characterized by tunnel structures and is common as well. Diffraction records of todorokite show the limited size of diffracting domains, and as a result of this, the broadening of diffraction lines for this mineral (estimated domain size is 8 μm).

The EDX microanalysis also showed probable schwertmannite (hydrated Fe oxide mineral with elevated content of sulphur) and yet unspecified oxyhydroxide of Al. In the case of locality 2 (Soběšovice) the association of secondary oxides and Mn oxyhydroxides (Fig. 4D) is somewhat different. Goethite in the fissures is covered with relatively rare max. 50 μm large crystals of manganite (Fig. 4E) and pyrolusite (Fig. 4F), and also abundant coatings composed of warped, extremely thin tabular grains. While manganite and pyrolusite were verified by powder X-ray diffraction analysis, coatings consisting of tabular grains are likely to be amorphous. Considering the elevated Ca content in EDX microanalyses it is possible to speculate on the occurrence of ranciéite.

Oxidation alterations in sideritic mudstones

Within the clasts of weathered mudstones, three zones can be distinguished. The outer zone is formed by a crust 1–2 cm thick, consisting of brown, relatively massive, macroscopically slightly thin-bedded material. According to the results of powder X-ray diffraction analysis, the major goethite is accompanied by chlorite and quartz. Microscopically, when compared with central parts of non-altered samples, the goethite forms pseudomorphs after siderite crystals. The content of pyrite is negligible.

The next is a 0.5–1 cm thick zone consisting of disintegrating powdery material of beige, beige-brown or reddish-brown colour shades. This zone also comprises intergrowths of goethite or hematite with an admixture of quartz, pyrite and chlorite.

The inner part of clasts is composed of unaltered matter of sideritic mudstone. Here, the siderite prevails and is accompanied by quartz. The content of chlorite and pyrite is lower than in the middle zone. Microscopically the samples of sideritic mudstone exhibit sparitic texture and consist of subhedral siderite crystals enclosed in the matrix. This matrix, according to the results of X-ray diffraction, is formed by chlorite and quartz. The latter mineral is also present as subhedral grains in the centre of siderite crystals. Pyrite is relatively abundant. This mineral in samples from locality 1 (Kunčice pod Ondřejníkem) is euhedral forming irregular grains up to 50 μm in size, while samples from locality 2 contain framboidal pyrite. Moreover, in samples from locality 2 (Soběšovice) thin layers with admixture of clastic material (silty grains of quartz) can be observed in some places. The powder X-ray diffraction analyses of sideritic mudstones from both localities indicate a presence of two differently substituted siderites (splitting of diffraction lines of siderite).

Discussion

The geochemical character of selenium largely resembles that of sulphur. Its form and/or its oxidation state in the system is determined by the pH-pε and/or (Eh) (De Cannière 2010). Based on the published pH-pε diagrams of the Se-O system (e.g. Olin et al. 2005; Cornelis et al. 2008) selenium may occur in four oxidation states, namely as Se(VI), Se(IV), Se(0) and Se(-II). Selenates and selenites are usually highly soluble in water and can be adsorbed on oxyhydroxides of Fe and Mn. In contrast, elemental Se(0) is characterized by an extremely low solubility. For instance, using thermodynamic modelling with software PhreeqC (Parkhurst & Appelo 1999, 2013) and with the LLNL database, it is possible to estimate the equilibrium concentration of 10^{-15} mol/l of Se(0) in pure water, pH = 7 and pε = 0.

The superposition of pH-pε diagrams of prevailing phases of both systems (Se-O, and/or Fe-O; see Fig. 5) shows a relatively large area of probable coexistence of crystalline Se(0) and goethite or Se(0) and amorphous $Fe(OH)_3$. This area lies in the section of geochemically quite realistic conditions (pH > 6 and pe approximately −3 to +5). A crucial factor responsible for the origin of Se is the maintaining of appropriate redox conditions, such as buffering by Fe^{2+}/Fe^{3+} ions.

Mingliang et al. (2011) refer to an interesting possibility for the origin of native Se(0). According to these authors, during an interaction between the solution containing seleni-

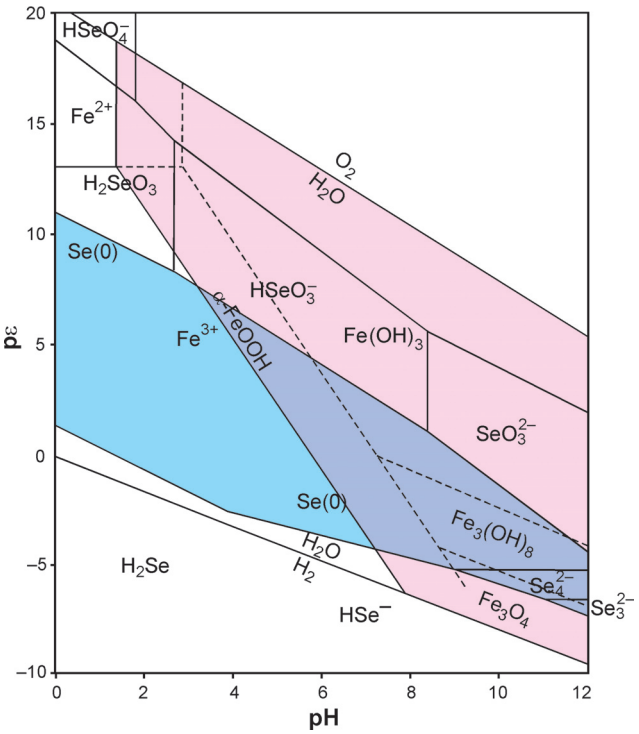

Fig. 5. Projection of pH-pε diagram of the Se-O system into the Fe-O system. Data for the system Se-O were taken from Olin et al. (2005), and apply to the total concentration of Se = 10^{-6} mol. The Fe-O system was constructed by using PhreeqC and/or Phreeplot program based on data from the LLNL thermodynamic database (Parkhurst & Appelo 1999, 2013; Kinninburgh & Cooper 2011) and applies to the total concentration of 10^{-4} mol/l Fe. Fields of predominance of solid phases (crystalline Se(0)) or goethite, amorphous $Fe(OH)_3$, $Fe_3(OH)_8$, and Fe_3O_4) are highlighted in both overlapping pH-pε diagrams. Lines bounding the field of stability of H_2O (line H_2O/H_2, resp. H_2O/O_2) are also included.

tes with pyrite, a reduction to Se(0) takes place in laboratory conditions. Similarly, it can also occur in some other phases capable of electron transfer, such as siderite, some other sulphides of Fe, magnetite or aluminosilicates containing Fe^{2+} (Brugemann 2005; Charlet 2007; Scheinost 2008). Scheinost & Charlet (2008) stated that the reduction of selenites or selenates by green rust, pyrite and ions of Fe^{2+} absorbed on montmorillonite is slow, kinetically limited (reaction that takes weeks); the reduction of selenites by mackinawite or magnetite with nanometric size is very quick (within one day). Scheinost & Charlet (2008) also stated, that a portion of selenites in solution may also be reduced by siderite of micron sizes. These authors also observed the occurrence of different reaction products (red and grey elemental Se, FeSe and Fe_7S_8). On the other hand, Mitchell et al. (2013) state that the crucial point and role in removing Se(IV) from solution in the presence of mineral phases is by adsorption, but no change in the oxidation state of Se was observed.

Szełęg et al. (2013) ascribe the formation of selenium crystals to bacterially induced oxidation of pyrite in a neutral environment and connect it with the presence of biogenic fibrous structures (reportedly bacteria of the genus *Leptothrix*). However, this genus includes strictly aerobic, chemoorganoheterotrophic bacteria which induce precipitation of Fe oxyhydroxides particularly in surface waters (Spring 2006). Therefore, the incidence of the occurrence of native selenium and the oxidation of pyrite with bacteria of the genus *Leptothrix* seem unlikely, but the bacterial influence on the origin of native Se at the described locality cannot in general be excluded either (Blum et al. 1998; Biswas et al. 2011).

The primary bond of selenium in rocks of the studied localities is not obvious, because the contents of Se in relatively abundant pyrite are below the detection limit of electron microanalysis. Literary sources state that in sedimentary rocks, Se is bound to sulphides and/or to organic matter. For example, Matamoros-Veloza et al. (2014) found that in shales, Se is bound especially to euhedral pyrite, in which it isomorphically replaces sulphur. In somewhat lower contents Se was found in framboidal pyrite as $FeSe_x$ phase.

With regard to the evidently crystalline character of selenium in fissures, this mineral is probably not produced by interfacial reactions between a solution and a solid phase or by direct precipitation. For this reason, the authors incline to the opinion that selenium in the studied localities is formed by gradual crystallization. Very probably microcrystalline barite, which was found in the locality of Kunčice pod Ondřejníkem, is a similarly formed accompanying phase. Barite also has an extremely limited solubility. It occurs very abundantly in fissures of weathered sediments (Matýsek, pers. observation).

The appearance of strongly weathered clasts of sideritic mudstones is a reminder of the initial stage of the formation of the so-called rattle stones (Van Loef 2000; Loope et al. 2012). This weathering structure that is relatively rare, especially in less weathered clasts of sideritic mudstone, is intersected by tiny secondary fissures of which walls are covered by thin coating of oxyhydroxides of Fe and Mn. Native selenium was detected in these tiny fissures. Changes in oxidation of beds of sideritic mudstones that lead to the formation of structures similar to the so-called rattle stones can be interpreted as a manifestation of acidification of siderite during contemporaneous diffusion transport of CO_2, Fe^{2+} or O_2. From the behaviour of siderite in the process of sulphidic weathering it is known that this mineral in oxidizing conditions is acid-base neutral (cf. Paktunc 1999). During the conversion of siderite to goethite the hydrogen ions in overall terms are not produced nor consumed. During the alteration of siderite its dissolution takes place (consumption of 2 moles of H^+/1 mol of siderite in formation of H_2CO_3). In the subsequent oxidation of Fe^{2+} to Fe^{3+}, 1 mol H^+/1 mol of Fe^{2+} is consumed. Finally, during the hydrolysis of Fe^{3+} to $Fe(OH)_3$ three moles of H^+ are released. Consequently, it is obvious that when alteration or transition of siderite into goethite takes place, the transport mechanisms of diffusion of H^+ (starting the dissolution and compensating for the losses of acidity) are the controlling factors towards the clast, while in the opposite direction the diffusion of O_2 or Fe^{+2} occurs. Nevertheless, it should be assumed that these diffusion flows are responsible for the formation of a concentric structure that will be stable over time and will be in balance.

Lithiophorite, which occurs in mudstone fissures, is commonly found in weathered zones of Mn deposits, ocean-floor manganese crust, some acid soils and low-temperature hydrothermal veins (Post & Appleman 1994; Jiang et al. 2007; Rao et al. 2010).

Acknowledgments: The study was carried out in the framework of the Project "Institute of clean technologies for the extraction and use of energy resources", reg. No. CZ.1.05/2.1.00/03.0082, supported by the Operational Program focused on Research and Development for Innovation, financed from EU structural funds and from the state budget. ED2.1.00/03.0082. The research was supported by Grant SP2014/10 financed by the Ministry of Education, Youth and Sports of the Czech Republic. We would like to thank Igor Broska (Bratislava, Slovakia), Eligiusz Szełęg (Sosnowiec, Poland) and Pavel Uher (Bratislava, Slovakia) for reading the manuscript, which was significantly improved by their critical remarks.

References

Anthony J.W., Bideaux R.A., Bladh K.W. & Nichols M.C. (Eds.). 1990: Handbook of mineralogy. Volume I. Elements, Sulfides, Sulfosalts. *Mineral Data Publishing*, Tuscon, Arizona, 1–813.

Biswas K.C., Barton L.L., Lok Tsui W., Shumana K., Gillespie J. & Eze Ch.S. 2011: A novel method for the measurement of elemental selenium produced by bacterial reduction of selenite. *J. Microbiol. Meth.* 86, 140–144.

Blum J.S., Bindi A.B., Buzzelli J., Stols J.F. & Oremland R.S. 1998: *Bacillus arsenioselenatis* sp. nov., and *Bacillus selenitireducens* sp. nov.: two haloalkaliphiles from Mono Lake, California that respire oxyanions of selenium and arsenic. *Arch. Microbiol.* 171, 19–30.

Bruggeman C., Maes A., Vancluysen J. & Vandemussele P. 2005: Selenite reduction in Boom clay: Effect of FeS_2, clay minerals and dissolved organic matter. *Environ. Pollut.* 137, 209–221.

Charlet L., Scheinost A.C., Tournassat C., Greneche J.M., Géhin A., Fernández-Martínez A., Coudert S., Tisserand D. & Brendle J. 2007: Electron transfer at the mineral/water interface: Selenium

reduction by ferrous iron sorbed on clay. *Geochim. Cosmochim. Acta* 71, 5731–5749.

Cornelis G., Johnson C.A., Van Gerven T. & Vandecasteele C. 2008: Leaching mechanisms of oxyanionic metalloid and metal species in alkaline solid wastes: A review. *Appl. Geochem.* 23, 955–976.

De Cannière P., Maes A., Williams S., Bruggeman Ch., Beauwens T., Maes N. & Cowper M. 2010: Behaviour of selenium in Boom clay. *External report of the Belgian Nuclear Research Centre.* SCK.CEN-ER-120, 10/PDC/P-9, 1–328.
Online: http://publications.sckcen.be/dspace/

Jiang X., Lin X., Yao D., Zhai S. & Guo W. 2007: Geochemistry of lithium in marine ferromanganese deposits. *Deep Sea Research* I, 54, 85–98.

Jianming Z., Wei Z., Xiaobing L., Shehong L. & Baoshan Z. 2004: Occurrence of native selenium in Yutangba and its environmental implications. *Appl. Geochem.* 19, 461–467.

Kaim A., Skupien P. & Jenkins R.G. 2013: A new Lower Cretaceous hydrocarbon seep locality from the Czech Carpathians and its fauna. *Palaeogeogr. Palaeoclimatol. Palaeoecol.* 390, 42–51.

Kinninburgh D.G. & Cooper D.M. 2011: User's guide to PhreePlot — Creating graphical output with PHREEQC, 1–588.
Online: http://www.phreeplot.org/

Loope D.L., Kettler R.M., Weber K.A., Hinrichs N.L. & Burgess D.T. 2012: Rinded iron-oxide concretions: hallmarks of altered siderite masses of both early and late diagenetic origin. *Sedimentology* 59, 1769–1781.

Malisa E.P. 2001: The behavior of selenium in geological processes. *Environ. Geochem. Hlth.* 23, 137–158.

Matamoros-Veloza A., Peacock C.L. & Benning L.G. 2014: Selenium speciation in framboidal and euhedral pyrites in shales. *Environ. Sci. Technol.* 48, 8972–8979.

Mingliang K., Fanrong C., Shijun W., Yongqiang Y., Bruggeman C. & Charlet L. 2011: Effect of pH on aqueous Se(IV) reduction by pyrite. *Environ. Sci. Technol.* 45, 7, 2704–2710.

Mitchell K., Couture R.-M., Johnson T.M., Mason P.R.D. & Van Cappellen P. 2013: Selenium sorption and isotope fractionation: Iron(III) oxides versus iron(II) sulfides. *Chem. Geol.* 342, 21–28.

Olin Å., Noläng Å., Öhman L.-O., Osadchii E. & Rosén E. 2005: Chemical thermodynamics of selenium. *Chemical Thermodynamics Series Volume 7. Nuclear Energy Agency, Elsevier Science*, Amsterdam, 1–851.

Paktunc A.D. 1999: Mineralogical constrains on the determination of neutralization potential and prediction of acid mine drainage. *Environmental Geol.* 39, 2, 103–112.

Parkhurst D.L. & Appelo C.A.J. 1999: User's guide to PHREEQC (Version 2): A computer program for speciation, batch-reaction, one-dimensional transport, and inverse geochemical calculations. *U.S. Geol. Surv.: Earth Science Information Center. Water-Resources Investigations Report* 99–4259, 1–326.

Parkhurst D.L. & Appelo C.A.J. 2013: Description of input and examples for PHREEQC version 3-A computer program for speciation, batch-reaction, one-dimensional transport, and inverse geochemical calculations: *U.S. Geol. Surv. Techniq. and Methods*, Book 6, Chap. A43, 1–497.
Online: http://pubs.usgs.gov/tm/06/a43/

Pavluš J. & Skupien P. 2014: Lower Cretaceous black shales of the Western Carpathians, Czech Republic: Palynofacies indication of depositional environment and source potential for hydrocarbons. *Mar. Petrol. Geol.* 57, 14–24.

Plant J.A., Kinniburgh D.G., Smedley P.L., Fordyce F.M. & Klinck B.A. 2013: Arsenic and selenium. In: Holland H.D. & Turekian K.K. (Eds.): Treatise on geochemistry. Vol. 9.02. *Elsevier*, New Orleans, 17–66.

Post J.E. & Appleman D.E. 1994: Crystal structure refinement of lithiophorite. *Amer. Mineralogist* 79, 370–374.

Post J.E., Heaney P.J. & Hanson J.C. 2003: Synchrotron X-ray diffraction study of the structure and dehydration behavior of todorokite. *Amer. Mineralogist* 88, 142–150.

Rao D.S., Nayak B.K. & Acharya B.C. 2010: Cobalt-rich lithiophorite from the Precambrian Eastern Ghats manganese ore deposit of Nishikhal, south Orissa, India. *Mineralogia* 41, 1–2, 11–21.

Scheinost A.C. & Charlet L. 2008: Selenite reduction by mackinawite, magnetite and siderite: XAS characterization of nanosized redox products. *Environ. Sci. Technol.* 42, 1984–1989.

Scheinost A.C., Kirsch R., Banerjee D., Fernández-Martínez A., Zaenker H., Funke H. & Charlet L. 2008: X-ray absorption and photoelectron spectroscopy investigation of selenite reduction by FeII-bearing minerals. *J. Contam. Hydrol.* 102, 228–245.

Skupien P., Smaržová A. & Měchová L. 2013: Palaeoenvironmental change in the Early Cretaceous Silesian Basin of the Western Carpathians (NE Czech Republic) inferred from palynological data. *Rev. Palaeobot. Palynol.* 197, 143–151.

Spring S. 2006: The genera *Leptothrix* and *Sphaerotilus*. In: Dworkin M., Falkow S., Rosenberg E., Schleifer K.-H. & Stackebrandt E. (Eds.): Prokaryotes. A handbook on the biology of bacteria. Vol. 5. Proteobacteria: Alpha and Beta Subclasses, Chapter 3.2.11. *Springer*, New York, 758–777.

Strawn D., Doner H., Zavarin M. & McHugo S. 2002: Microscale investigation into the geochemistry of arsenic, selenium, and iron in soil developer in pyritic shale materials. *Geoderma* 108, 237–257.

Szełęg E., Janeczek J. & Metelski P. 2013: Native selenium as a byproduct of microbial oxidation of distorted pyrite crystals: the first occurrence in the Carpathians. *Geol. Carpathica* 64, 3, 231–236.

Tolu J., Thiry Y., Bueno M., Jolivet C., Potin-Gautier M. & Le Hécho I. 2014: Distribution and speciation of ambient seleniumin contrasted soils, from mineral to organic rich. *Sci. Total Environ.* 479–480, 93–101.

Van Loef J.J. 2000: Composition and genesis of rattlestones from Dutch soils as shown by Mössbauer spectroscopy, INAA and XRD. *Geol. En. Mijnb. N.J.G.* 79, 1, 59–71.

Yang H., Lu R., Downs R.T. & Costin G. 2006: Goethite, a-FeO(OH), from single-crystal data. *Acta Crystallographica* E62, i250–i252.